

# Comparison of entanglement generation rates between continuous and discrete variable repeaters

Josephine Dias,<sup>1,\*</sup> William J. Munro,<sup>2,3</sup> T.C. Ralph,<sup>1</sup> and Kae Nemoto<sup>3</sup>

<sup>1</sup>*Centre for Quantum Computation and Communication Technology,  
School of Mathematics and Physics, University of Queensland, Brisbane, Queensland 4072, Australia.*

<sup>2</sup>*NTT Basic Research Laboratories & NTT Research Center for Theoretical Quantum Physics,  
NTT Corporation, 3-1 Morinosato-Wakamiya, Atsugi, Kanagawa, 243-0198, Japan.*

<sup>3</sup>*National Institute of Informatics, 2-1-2 Hitotsubashi, Chiyoda, Tokyo 101-0003, Japan.*

(Dated: June 17, 2019)

Quantum repeaters are a well known method to overcome the exponential photon loss scaling that quantum states acquire as they are transmitted over long distances. While repeaters for discrete variable encodings of quantum information have existed for some time, novel approaches for continuous variable encoding quantum repeaters have recently been proposed. In this work, we present a method of utilising a discrete variable repeater protocol to distribute continuous variable states and then utilize this to compare the rates of continuous variable entanglement distribution between first generation continuous and discrete variable repeaters.

## I. INTRODUCTION

The development of technologies according to the principles of quantum mechanics allows promising real world applications including secure communication [1, 2] and quantum information transfer [3]. However, utilising these technologies over long distances remains challenging due to fiber loss or free space attenuation [4]. A proposed method for allowing the long distance distribution of quantum states are quantum repeaters [5]. In this model, the long distance is segmented into smaller, more manageable attenuation lengths. Entanglement is distributed along these lengths followed by nested entanglement purification [6] and swapping [7]. By using a quantum repeater, the exponential error probability scaling with distance that would arise from direct transmission, can be overcome [8].

Repeater protocols have existed for discrete-variable (DV) encoding since the late nineties [5], and have been through various iterations of protocol improvements since then [4, 9]. The evolution of quantum repeater protocols has been broadly categorised into three distinct generations [9, 10]. First generation repeaters are characterised by their use of heralded entanglement generation between repeater nodes, and nested entanglement purification protocols [5, 11]. While first generation repeater protocols were limited due to the time associated with two-way communication of successful generation and purification, second [12–14] and third [15–18] generation protocols utilise quantum error correction to be much more efficient.

Recently, there have been three different proposals for repeater protocols that work with continuous variable (CV) encodings for the first time [19–21]. The DV and CV regimes of quantum information are subject to their

own unique advantages and disadvantages. It is of significant interest therefore, how these first generation continuous variable quantum repeaters perform compared to existing discrete variable counterparts.

This work aims to answer this question by performing a comparison between first generation CV and DV repeaters. It is important to compare the recently published first generation CV repeaters [19, 20] to first generation DV repeaters [5] so as not to mar the comparison by enabling the rates of the DV repeaters to benefit from the large body of literature that has improved upon these protocols since their inception [4, 9, 10]. We will compare how efficient both CV and DV repeaters can distribute CV entangled resource states. The performance metric we will use is the *repeater rate*  $R_{\text{Rep}}$  for the generation of entangled states. To ensure a fair comparison we will compare the repeater rates of both repeaters sending the same state, and receiving states of similar entanglement level. Both repeaters will be modelled sending a two-mode squeezed vacuum (otherwise known as an Einstein-Podolsky-Rosen state [22, 23]) of form

$$|\chi\rangle = \sqrt{1-\chi^2} \sum_{n=0}^{\infty} \chi^n |n\rangle |n\rangle, \quad (1)$$

where  $\chi$  controls the strength of the squeezing. A basic conceptual diagram of the comparison is shown in Figure 1. This paper is arranged in the following way: in Section II we review the discrete variable repeater protocol, we will also illustrate how it can be used to distribute continuous variable quantum states. In Section III we review the continuous variable repeater protocol from Ref. [19]. We discuss specifics of the rate comparison and present results in Section IV before we summarize and conclude.

\* josephine.dias@uqconnect.edu.au

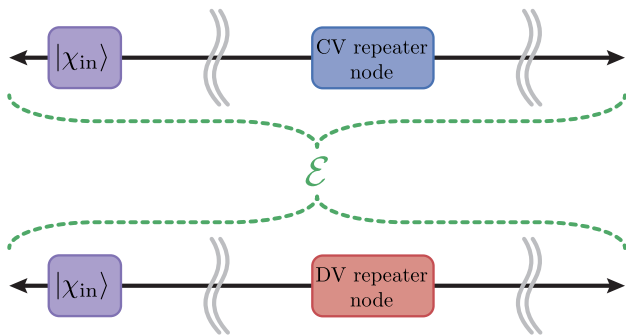


FIG. 1. Basic set up. We compare rates of pair production between CV and DV repeater protocols, ensuring that the initial and distributed states have the same amount of entanglement.

## II. DISCRETE VARIABLE REPEATERS

The 1998 paper by *Briegel et al.* was the first to present the concept of a quantum repeater with the goal of overcoming the exponential loss scaling and creating an entangled pair over arbitrary large distances [5]. The Briegel model, now known as a first generation quantum repeater, consists of three elements: entanglement distribution, entanglement swapping [7] and nested purification protocols [6]. The protocol begins by distribution of a number of entangled pairs between adjacent nodes in the repeater network. Ideal operation of the repeater would achieve distribution of perfect Bell pairs between nodes,

$$|\Phi^+\rangle = \frac{1}{\sqrt{2}}(|0\rangle|0\rangle + |1\rangle|1\rangle), \quad (2)$$

that would then be used for subsequent rounds of entanglement swapping until a final pair is produced between both ends of the channel. This ideal situation is unrealistic however, due to the imperfect local operations at pair production. A possible model for the errors induced by imperfect production is the Werner state [24]:

$$\hat{\rho}_W = \frac{4F-1}{3} |\Phi^+\rangle \langle \Phi^+| + \frac{1-F}{3} \mathbb{I}_4 \quad (3)$$

which has fidelity  $F$  for the required pair  $|\Phi^+\rangle$  but also contains a mixture of all the other Bell states. With two pairs (labelled  $\hat{\rho}_{W_{12}}, \hat{\rho}_{W_{34}}$ ) distributed between three nodes, entanglement swapping proceeds as follows: a local joint Bell-state measurement is conducted between qubits 2 and 3. The results of that measurement are then sent via a classical communication channel to qubit 4 where a Pauli correction is made on qubit 4 based on the outcome of the measurement. The result being, a single entangled pair is now shared between the outer nodes  $\hat{\rho}_{W_{14}}$ . Beginning with two Werner pairs, each of fidelity

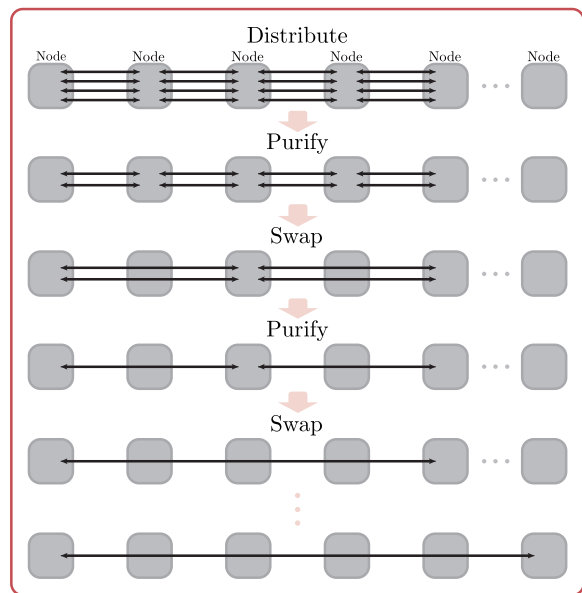


FIG. 2. Quantum repeater for discrete variables. This illustration shows how the repeater protocol from Ref. [5] may operate. Beginning with the initial entanglement distribution of many entangled pairs between each node, subsequent rounds of entanglement purification and swapping follow resulting in a single entangled pair held between both ends of a long distance channel.

$F$ , the fidelity of the swapped pair is given by [9]:

$$F_{swap} = F^2 + \frac{(1-F)^2}{3}, \quad (4)$$

which is always less than the fidelity of the initial pair  $F$ . In this way, as the channel length increases so too does the number of repeater nodes and therefore the number of swapping operations that need to be performed. To prevent degradation of entanglement from the entanglement swapping operations, entanglement purification protocols are necessary.

Entanglement purification proceeds by distributing two pairs between two repeater nodes. Within each node, a unitary is applied to the qubit of one pair and the qubit of the second. Following the unitary operations, one of the pairs is measured out and first entangled pair is kept if the measurement results are the same and discarded if the measurement results are different. In this way, two entangled pairs of fidelity  $F$  can result in a single entangled pair of fidelity [6]:

$$F_{pur} = \frac{F^2 + \frac{1}{9}(1-F)^2}{F^2 + \frac{2}{3}(1-F) + \frac{5}{9}(1-F)^2} \quad (5)$$

where the fidelity of the purified pair  $F_{pur}$  is higher than that of the initial two pairs. Entanglement purification is probabilistic however, and the probability of successful purification depends on the fidelity of the initial pairs [6],

$$P_{pur} = F^2 + \frac{2}{3}(1-F) + \frac{5}{9}(1-F)^2. \quad (6)$$

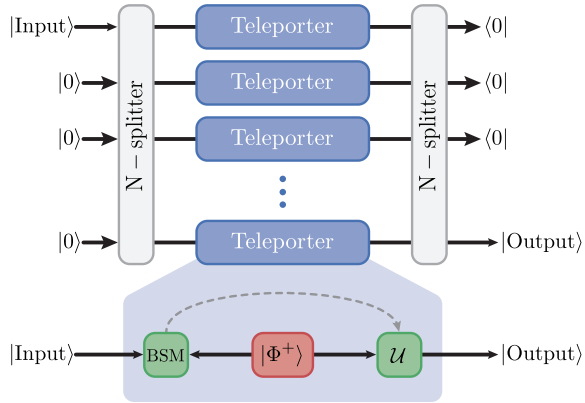


FIG. 3. Teleporting CV states using DV entangled resources using the protocol from Ref.[25].

Therefore, while entanglement swapping may be used to distribute entanglement over a long channel using many repeater nodes, the unfortunate consequence of using imperfect pairs means fidelity will degrade for longer channels. Entanglement purification is required to circumvent this, the cost being the wait time for the purification to succeed and the extra entangled pairs that are needed.

In operating the entire repeater, the number of pairs initially distributed will depend on both the number of nodes along the channel and the fidelities of the required final pair and the initial distributed pairs. As an example of how the entire repeater protocol might operate consider Figure 2. The protocol begins by distributing many different copies of entangled pairs between the nodes. The initial distribution is followed by one round of purification, taking two entangled pairs to a single entangled pair of higher fidelity. A Bell-state measurement is conducted at the second and fourth nodes and after the correction depending on the measurement outcome, entanglement is held between the first and third nodes and the third and fifth nodes. Further rounds of entanglement purification and swapping follow. After all rounds of purification and swapping have succeeded, entanglement is held between both ends of the long channel.

### A. Teleporting CV states using DV resources

Using the DV repeater protocol outlined in the previous section, we may achieve distribution of discrete variable entangled resource states. By employing a specific teleportation protocol, we may use these entangled resource states to teleport any continuous variable quantum state. This teleportation protocol, conceived by Andersen and Ralph in 2011 [25], is pictured in Figure 3 and proceeds as follows: an input CV state to be teleported is split on an array of beam splitters (N-splitter) which splits the state evenly among many different modes. The

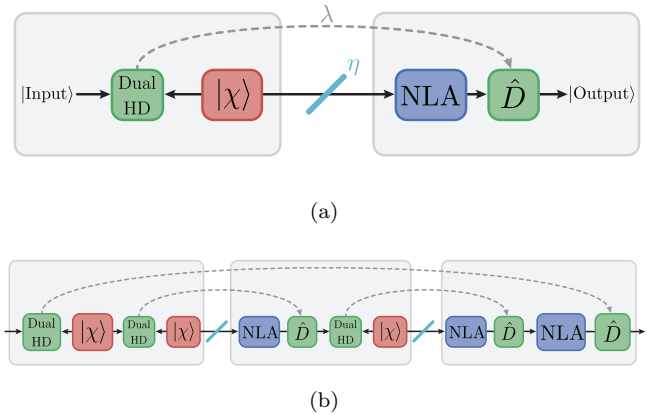


FIG. 4. Quantum repeater for continuous variables.(a) CV error correction protocol from Ref. [26]. (b) The CV repeater is constructed by nesting CV error correction protocols. Here, the simplest nesting level is shown comprising of 2 links of the repeater (1 repeater node).

number of modes is dependent on the size (average photon number) of the input state. Each mode is then input into its own discrete teleportation protocol (pictured in the blue inset in Figure 3). Here, Bell states are distributed between both ends of the channel. The sender mixes each of the modes with their qubit of the Bell state and conducts a Bell-state measurement. The results of the measurement are communicated classically to the receiver who then conducts a unitary operation to the other qubit of the entangled pair. This results in each reduced amplitude mode being teleported individually. After successful teleportation of all the modes, they are then coherently recombined on an N-splitter. When all the ports of the N-splitter register  $|0\rangle$ , the output state has been recombined and the teleportation is successful.

## III. CONTINUOUS VARIABLE REPEATERS

We now briefly review the CV repeater protocol from Ref. [19]. Like its discrete variable counterpart, the CV repeater from Ref. [19] contains entanglement distribution, entanglement swapping and entanglement distillation. However, each of these elements are different from the previously described discrete versions so as to be compatible with continuous variable encodings of quantum information.

This repeater protocol is based on an earlier error correction protocol for CV states against loss [26] and is constructed by concatenating error correction protocols. To illustrate how the repeater works, we will first describe how the error correction protocol works, pictured in Figure 4(a). The protocol begins by distributing CV entangled resource states between ends of the channel (or nodes of the repeater). These entangled resources states are the two-mode squeezed vacuum states given in (1).

Distribution of these states is performed asymmetrically with one arm of the entangled state passing through the lossy channel while the other arm of the entangled state remains in the repeater node. Entanglement distillation is performed on the arm of the entanglement that has been decohered by loss via the Noiseless Linear Amplifier (NLA) [27]. After successful operation of the NLA, the input state is teleported using CV teleportation [28]. This protocol works to correct errors induced by loss on Gaussian states by effectively reducing the amount of attenuation the state is subjected to.

For increasing channel lengths, these error correction protocols are strung together sequentially in pairs and then nested in another error correction protocol. This is shown in Figure 4(b) where the simplest nesting level of the repeater with two links (or one repeater node) is pictured. In this setup, two error correction protocols are operated sequentially on each link of the channel. Once both herald successful operation of their NLAs, they may then operate the NLA at the higher level of error correction. Scaling up the distance further requires higher nesting levels as explained in Ref. [19].

#### IV. RATE COMPARISON

We have now reviewed all the protocols utilised in our comparison of DV and CV repeater rates. Our goal in this work is to compare the rate of distribution of CV entanglement (rather than QKD key rates) that can be achieved using CV and DV resources. While there are many factors that can affect performance of the repeaters that cannot be directly compared between CV and DV regimes, our efforts to make the comparison fair will be outlined in this section.

Firstly, inputs states to both repeaters will be two-mode Gaussian squeezed states of the same squeezing  $\chi$ . Distribution of these states using the DV repeater will follow the protocol pictured in Figure 5(a), whereby the DV repeater is used to generate entangled pairs between ends of the channel, and those entangled pairs are then used for teleportation of the CV input state. It worthwhile to note that teleportation of CV states in this way requires multiple modes if the average photon number is greater than 1. Therefore, this approach will require many DV repeaters running in parallel to achieve distribution of CV states of high mean photon number.

We are comparing the DV repeater distribution protocol pictured in Figure 5(a) to the CV protocol in Figure 5(b). Here the CV repeater is used to generate entanglement between both ends of the channel which is then used for teleportation of the input two-mode squeezed state. While the entangled states in both regimes will be decohered somewhat due to the elements in the repeater, we are comparing situations where the inputs to both repeaters have the same squeezing  $\chi$  and the output of both DV and CV protocols have the same amount of entanglement. The entanglement measure we use in this

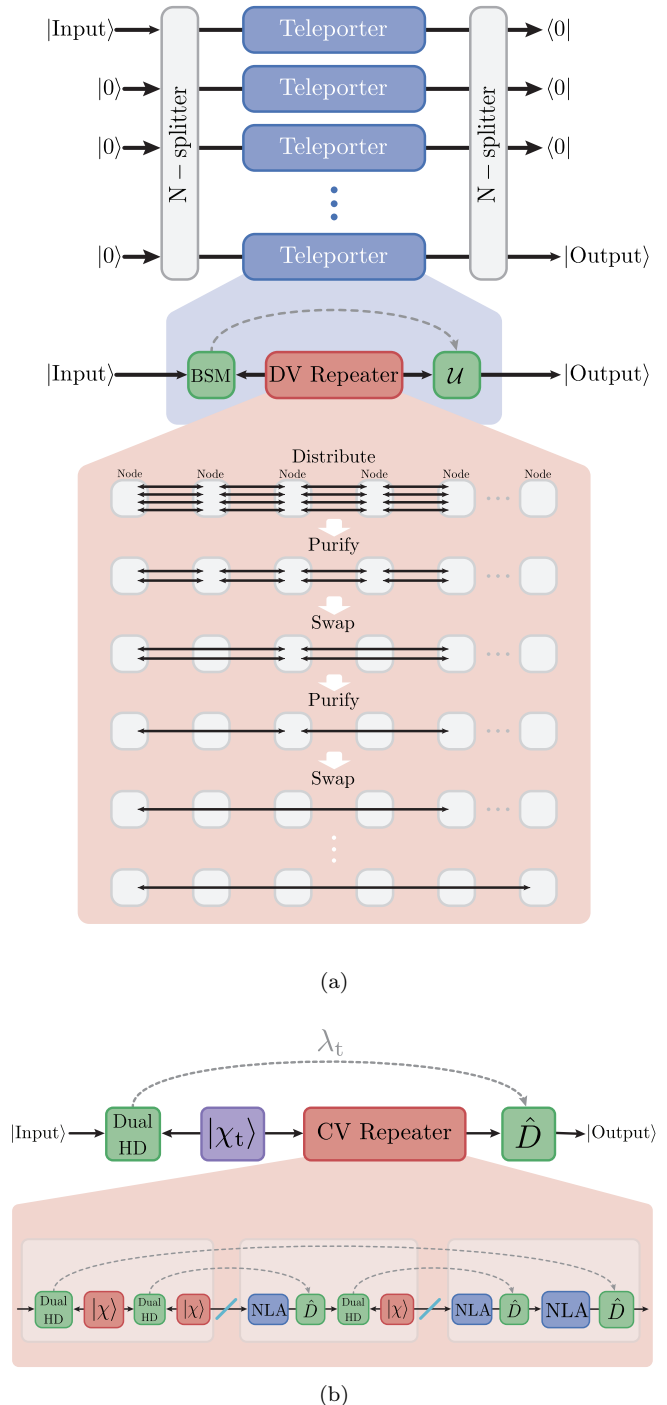


FIG. 5. Distributing CV entangled states using CV and DV repeaters. (a) Protocol to distribute CV states using discrete entangled resources. (b). CV repeater nested within a CV teleportation protocol.

work is the entanglement of formation [29].

While the operations that take place at each node are different for the CV and DV protocols, we approximately allocate the same resources to both repeaters by ensur-

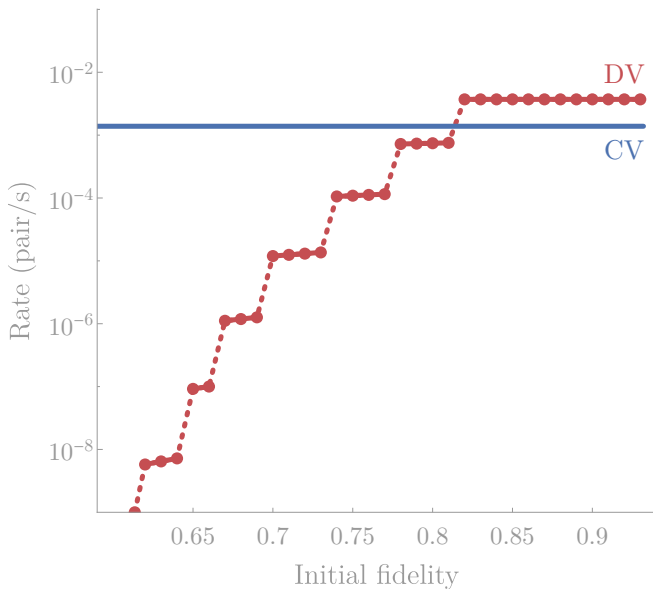


FIG. 6. Repeater rates of first generation DV and CV repeaters operating over 400km. The blue line represents the rate achieved by the CV repeater with 2 links. The red dot points represent the rate achieved by the DV repeater operating with a variety of initial fidelities of the entangled pairs distributed between nodes. Results here are for a required fidelity of the final pair of  $F_{req} = 0.67$  which has been chosen to ensure DV and CV repeaters produce states of the same entanglement of formation. Discrete jumps in the DV repeater rate are attributed to the discrete number of purification rounds. The required number of purification rounds depends on the initial fidelity and required fidelity. Both DV and CV repeaters take an input state of  $\chi = 0.5$ .

ing we compare the same number of nodes. As we are using the CV repeater from Ref. [19] in our comparison, we note that results from this repeater are only available for the 2 link (1 repeater node) case. Results for higher numbers of channel links, corresponding to higher nesting levels of the error correction protocol, are left for future consideration. For this reason, our comparison also restricts the DV repeater results to only 2 links. It is still interesting to consider, in this constrained case of only allowing a single repeater node, which distribution protocol is more efficient.

Additionally, we make a number of idealised assumptions about both protocols including photon sources and detectors of perfect efficiencies and infinite memory coherence time. We also only assume linear optics capabilities with these rate comparisons. Our comparison also takes into account the time needed for classical communication of successful results and allowing all probabilistic operations to succeed assuming finite resources. This was achieved following the methods in Refs. [30] and [31] respectively.

Given the previously outlined assumptions and restrictions on this comparison, we present in Figure 6 the *repeater rate*, in units of entangled pairs per second sent

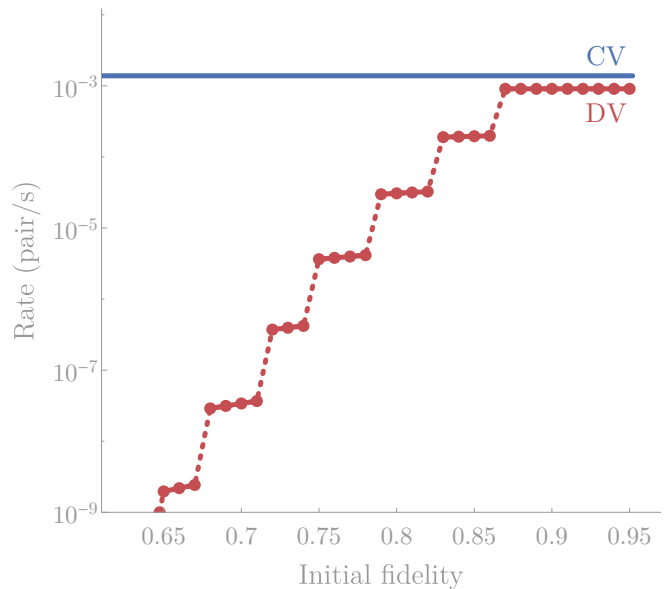


FIG. 7. Repeater rates of first generation DV and CV repeaters operating at 400km with both DV and CV repeaters taking an input state of  $\chi = 0.9$ . The blue line represents the rate achieved by the CV repeater. The red dot points represent the rate achieved by the DV repeater. To ensure the CV and DV repeaters distribute states of the same entanglement of formation, the required fidelity for the DV repeater has been set to  $F_{req} = 0.74$ .

over a distance of 400km. Here, we have modelled both the DV protocol and the CV protocol (both operating with a single repeater node) sending a two-mode squeezed state of  $\chi = 0.5$  to result in the same entanglement of formation  $\mathcal{E} \approx 0.14$  between both output states. As the average photon number of one arm of this two-mode squeezed state is less than one ( $\bar{n} \approx 0.33$ ), results in Figure 6 present the DV teleporter operating on one mode only.

In this result, we are varying the fidelity of the initial pairs of Werner states distributed between the nodes and comparing resulting rates of entanglement distribution to the CV rate. As the initial fidelity is increased, the number of rounds of purification needed to achieve the correct required fidelity of the final pair is reduced and therefore the rate is increased. The required fidelity for Figure 6 is  $F_{req} = 0.67$  and has been chosen so as to ensure the DV and CV repeaters produce output states with the same entanglement of formation. In this case, an initial fidelity of  $F_i \geq 0.82$  is required for the entanglement distribution rate of the DV protocol to surpass that of the CV protocol.

It is also interesting to note how the comparison performs as the size of the CV state we are distributing scales up. The low average photon number of the two-mode Gaussian squeezed state used in the comparison for Figure 6 permitted use of only one mode in the DV distribution protocol. However, for a higher energy state using only one mode would not accurately enough recreate the

original state after teleportation.

For this case, we present the result in Figure 7 in which both the CV and DV repeaters transmit a two-mode squeezed state of  $\chi = 0.9$  again over 400km. This input state has an average photon number of  $\bar{n} \approx 4.2$  and therefore, 4 modes are required to distribute a state of this size using DV resources via the protocol described in Figure 5(a). Again, the results presented in Figure 7 ensure CV and DV outputs have the same entanglement of formation ( $\mathcal{E} \approx 0.35$ ), with the required fidelity for the DV repeater being set to  $F_{req} = 0.74$  to achieve this. It can be seen that even as the fidelity of the initial pairs distributed within the DV repeater is increased to  $F_i = 1$ , the DV distribution rate does not surpass that of the CV repeater. When the initial fidelity reaches a certain point  $F_i \geq 0.87$  the rate plateaus because even with a high enough initial fidelity so as to not require any purification rounds, the distribution rate is still not high enough to beat the CV rate.

It should be noted that while some optimisation of the CV repeater has been done to achieve the results presented in this paper, the CV repeater remains not yet fully optimised. It is expected that with further progress modelling the operation of the repeater, the CV repeater rates could be increased further. Additionally, we note that the conclusions that can be drawn from this work are limited as more results at higher link numbers are necessary to draw conclusions about how the performance of the repeaters scale with distance.

Nevertheless, we hope that this result highlights how DV resources may be effectively utilised to distribute CV states. We note that DV repeaters may be efficiently employed to distribute CV states with low average energy, but for higher average energy states in this specific case, they may not be as efficient as first generation CV repeaters. Further we expect significant performance increases as the second and third generation CV repeater schemes are developed.

- 
- [1] N. Gisin, G. Ribordy, W. Tittel, and H. Zbinden, *Rev. Mod. Phys.* **74**, 145 (2002).
- [2] V. Scarani, H. Bechmann-Pasquinucci, N. J. Cerf, M. Dušek, N. Lütkenhaus, and M. Peev, *Rev. Mod. Phys.* **81**, 1301 (2009).
- [3] S. Pirandola, J. Eisert, C. Weedbrook, A. Furusawa, and S. L. Braunstein, *Nat. Photonics* **9**, 641 (2015).
- [4] N. Sangouard, C. Simon, H. de Riedmatten, and N. Gisin, *Rev. Mod. Phys.* **83**, 33 (2011).
- [5] H.-J. Briegel, W. Dür, J. I. Cirac, and P. Zoller, *Phys. Rev. Lett.* **81**, 5932 (1998).
- [6] C. H. Bennett, G. Brassard, S. Popescu, B. Schumacher, J. A. Smolin, and W. K. Wootters, *Phys. Rev. Lett.* **76**, 722 (1996).
- [7] M. Żukowski, A. Zeilinger, M. A. Horne, and A. K. Ekert, *Phys. Rev. Lett.* **71**, 4287 (1993).
- [8] L.-M. Duan, M. D. Lukin, J. I. Cirac, and P. Zoller, *Nature* **414**, 413 (2001).
- [9] W. J. Munro, K. Azuma, K. Tamaki, and K. Nemoto, *IEEE J. Sel. Topics Quantum Electron.* **21**, 78 (2015).
- [10] S. Muralidharan, L. Li, J. Kim, N. Lütkenhaus, M. D. Lukin, and L. Jiang, *Sci. Rep.* **6**, 20463 (2016).
- [11] W. Dür, H.-J. Briegel, J. I. Cirac, and P. Zoller, *Phys. Rev. A* **59**, 169 (1999).
- [12] L. Jiang, J. M. Taylor, K. Nemoto, W. J. Munro, R. Van Meter, and M. D. Lukin, *Phys. Rev. A* **79**, 032325 (2009).
- [13] W. J. Munro, K. A. Harrison, A. M. Stephens, S. J. Devitt, and K. Nemoto, *Nat. Photonics* **4**, 792 (2010).
- [14] M. Zwerger, H. J. Briegel, and W. Dr, *Sci. Rep.* **4**, 5364 (2014).
- [15] W. J. Munro, A. M. Stephens, S. J. Devitt, K. A. Harrison, and K. Nemoto, *Nat. Photonics* **6**, 777 (2012).
- [16] A. G. Fowler, D. S. Wang, C. D. Hill, T. D. Ladd, R. Van Meter, and L. C. L. Hollenberg, *Phys. Rev. Lett.* **104**, 180503 (2010).
- [17] S. Muralidharan, J. Kim, N. Lütkenhaus, M. D. Lukin, and L. Jiang, *Phys. Rev. Lett.* **112**, 250501 (2014).
- [18] K. Azuma, K. Tamaki, and H.-K. Lo, *Nat. Commun.* **6**, 6787 (2015).
- [19] J. Dias and T. C. Ralph, *Phys. Rev. A* **95**, 022312 (2017).
- [20] F. Furrer and W. J. Munro, *Phys. Rev. A* **98**, 032335 (2018).
- [21] K. P. Seshadreesan, H. Krovi, and S. Guha, in *Conference on Lasers and Electro-Optics* (Optical Society of America, 2019) p. FTh4A.5.
- [22] A. Einstein, B. Podolsky, and N. Rosen, *Phys. Rev.* **47**, 777 (1935).
- [23] C. Weedbrook, S. Pirandola, R. García-Patrón, N. J. Cerf, T. C. Ralph, J. H. Shapiro, and S. Lloyd, *Rev. Mod. Phys.* **84**, 621 (2012).
- [24] R. F. Werner, *Phys. Rev. A* **40**, 4277 (1989).
- [25] U. L. Andersen and T. C. Ralph, *Phys. Rev. Lett.* **111**, 050504 (2013).
- [26] T. C. Ralph, *Phys. Rev. A* **84**, 022339 (2011).
- [27] T. C. Ralph and A. P. Lund, *AIP Conference Proceedings* **1110**, 155 (2009), <https://aip.scitation.org/doi/pdf/10.1063/1.3131295>.
- [28] S. L. Braunstein and H. J. Kimble, *Phys. Rev. Lett.* **80**, 869 (1998).
- [29] P. Marian and T. A. Marian, *Phys. Rev. Lett.* **101**, 220403 (2008).
- [30] S. Bratzik, S. Abruzzo, H. Kampermann, and D. Bruß, *Phys. Rev. A* **87**, 062335 (2013).
- [31] N. K. Bernardes, L. Praxmeyer, and P. van Loock, *Phys. Rev. A* **83**, 012323 (2011).